CDF/PUB/BOTTOM/PUBLIC/9352

PRL Draft 3.0

Measurement of Resonance Parameters of Orbitally Excited Narrow B^0 Mesons

The CDF Collaboration

Abstract

We report a measurement of resonance parameters of the orbitally excited ($L = 1$) narrow B^0 mesons in decays to $B^{(*)+}\pi^-$ using 1.7 fb^{-1} of data collected by the CDF II detector at the Fermilab Tevatron. The mass and width of the B_2^{*0} state are measured to be $m(B_2^{*0}) = 5740.2^{+1.7}_{-1.8}(\text{stat.})^{+0.9}_{-0.8}(\text{syst.})$ MeV/c^2 and $\Gamma(B_2^{*0}) = 22.7^{+3.8}_{-3.2}(\text{stat.})^{+3.2}_{-10.2}(\text{syst.})$ MeV/c^2. The mass difference between the B_2^{*0} and B_1^0 states is measured to be $14.9^{+2.2}_{-2.5}(\text{stat.})^{+1.2}_{-1.4}(\text{syst.})$ MeV/c^2, resulting in a B_1^0 mass of $5725.3^{+1.6}_{-2.2}(\text{stat.})^{+1.4}_{-1.5}(\text{syst.})$ MeV/c^2. This is currently the most precise measurement of the masses of these states and the first measurement of the B_2^{*0} width.

PACS: 14.40.Nd, 12.40.Yx

Mesons consisting of a light and a heavy quark are an interesting laboratory for the study of quantum chromodynamics, the theory of strong interactions. The role of the heavy-light quark mesons is similar to that played by the hydrogen atom in understanding quantum electrodynamics. The bound states of a $\bar{b}$ quark with either a light u or d quark are referred to as B mesons. The states with zero internal orbital

angular momentum ($L = 0$) and spin parity $J^P = 0^-$ (B) and 1^- (B^*) are well established [1], but the spectroscopy of the orbitally excited B states has not been well studied. For $L = 1$, the total angular momentum of the light quark is $j = \frac{1}{2}$ or $j = \frac{3}{2}$. With the addition of spin of the heavy quark, two doublets of states are expected: states with $j = \frac{1}{2}$, named B_0^* ($J = 0$) and B_1' ($J = 1$), and states with $j = \frac{3}{2}$, named B_1 ($J = 1$) and B_2^* ($J = 2$). These four states are collectively referred to as B^{**}.

Heavy quark effective theory [2] predicts that the mass splitting within each doublet of a heavy-light quark meson is inversely proportional to the heavy quark mass [2–8]. The $j = \frac{1}{2}$ states are expected to decay to $B^{(*)}\pi$ via an S-wave transition and to exhibit resonance widths in the range $100 - 200$ MeV/c^2 [9]. The $j = \frac{3}{2}$ states are expected to decay to $B^{(*)}\pi$ via a D-wave transition and to have widths of $10 - 20$ MeV/c^2 [7,8]. This Letter focuses on the B_1 and B_2^* observed in $B\pi$ final states. The decay $B_1 \to B\pi$ is forbidden by conservation of angular momentum and parity, while both $B_2^* \to B\pi$ and $B_2^* \to B^*\pi$ decays are allowed. Decays to a B^* are followed by $B^* \to B\gamma$, where the photon is not reconstructed in CDF due to its low energy. Because of the missing photon, the measured $B\pi$ mass in $B_1 \to B^*\pi \to B\pi\gamma$ and $B_2^* \to B^*\pi \to B\pi\gamma$ events is lower than the $B^*\pi$ mass by 45.78 ± 0.35 MeV/c^2 [1], resulting in an expected signal structure of three narrow $B\pi$ peaks for the B_1 and B_2^*.

Previous measurements of properties of the $j = \frac{3}{2}$ B_1^0 and B_2^{*0} mesons using inclusive or partially reconstructed decays did not separate the narrow states [10, 11] or were limited by low sample statistics [12]. Recently the D0 Collaboration resolved the B_1^0 and B_2^{*0} masses [13]. The superb mass resolution of the CDF II detector allows better precision and enables us to measure the B_2^{*0} width. Here, we present measurements of the masses of the B_1^0 and B_2^{*0} states and the width of the B_2^{*0} state. We reconstruct B^{**0} in $B^+\pi^-$ and $B^{*+}\pi^-$ decays, where the B^+ candidates decay into $J/\psi K^+$, $\bar{D}^0\pi^+$, and $\bar{D}^0\pi^+\pi^+\pi^-$ final states with $J/\psi \to \mu^+\mu^-$ and $\bar{D}^0 \to K^+\pi^-$. Throughout this paper, any reference to a specific charge state implies the charge conjugate state as

well.

We use a data sample of events produced in $p\bar{p}$ collisions at $\sqrt{s} = 1.96$ TeV recorded by the CDF II detector at the Tevatron, corresponding to an integrated luminosity of 1.7 fb^{-1}. The components and performance parameters of CDF II [14] most relevant for this analysis are the tracking, the muon detectors, and the trigger on displaced vertices. The tracking system lies in a uniform axial magnetic field of 1.4 T. The inner tracking volume up to a radius of 28 cm contains 7 layers of double-sided silicon microstrip detectors [15] outside a layer of single-sided silicon mounted directly on the beam pipe at a radius of 1.5 cm. This system provides excellent resolution of the impact parameter, d_0, defined as the distance of closest approach of the track to the interaction point in the transverse plane. The outer tracking volume contains an open-cell drift chamber (COT) up to a radius of 137 cm [16]. Muons are detected in planes of drift tubes and scintillators [17] located outside the hadronic and electromagnetic calorimeters. The muon detectors used in this study cover the pseudorapidity range $|\eta| \leq 1.0$, where $\eta = -\ln\tan(\theta/2)$ and θ is the polar angle measured from the proton beam.

A three-level trigger system selects events in real time. A dimuon trigger [14] requires two tracks of opposite charge that match track segments in the muon chambers and have a combined dimuon mass consistent with the J/ψ mass. An extremely fast tracker at level 1 (XFT) [18] groups COT hits into tracks in the transverse plane. A silicon vertex trigger at level 2 (SVT) [19] adds silicon hits to tracks found by the XFT, thus providing better-defined tracks and allowing candidate selection based on the impact parameter. A displaced vertex trigger [20] requires two tracks each with a transverse momentum magnitude, p_T, greater than 2 GeV/c and with $0.12 < d_0 < 1$ mm. Additionally, the intersection point of the track pair must be transversely displaced from the $p\bar{p}$ interaction point by at least 0.2 mm, and the pair must have a scalar sum $p_T(1) + p_T(2) > 5.5$ GeV/c.

Decays $B^+ \to J/\psi K^+$ are reconstructed from the dimuon trigger data while decays $B^+ \to \bar{D}^0\pi^+(\pi^+\pi^-)$ are reconstructed from the displaced vertex trigger data. In each decay, the tracks are constrained in a three-dimensional kinematic fit to the appropriate B^+ vertex topology with the J/ψ and $\bar{D}^0$ masses constrained to the world average values [1]. Each track from the same interaction point as the B^+ and not used to reconstruct the B^+ is considered as a pion candidate, and its 4-momentum is combined with that of the B^+ candidate to form a B^{**0} candidate. We search for narrow resonances in the mass difference distribution of $Q = m(B^+\pi^-) - m(B^+) - m_\pi$, where $m(B^+\pi^-)$ and $m(B^+)$ are the reconstructed invariant masses of the $B^+\pi^-$ pair and the B^+ candidate, and m_π is the pion mass.

The B^+ candidates are selected using independent artificial neural networks for each of the three B^+ decay modes. The neural networks are based on the NeuroBayes package [21]. For the decays $B^+ \to J/\psi K^+$ and $B^+ \to \bar{D}^0\pi^+$, we use the training and selection methods developed in Ref. [22]. For the decay $B^+ \to \bar{D}^0\pi^+\pi^+\pi^-$ we closely follow the construction of the neural networks for the other two decays. To train this last neural network we use data from the region $5325 < m(B^+) < 5395$ MeV/c^2 as the background sample and simulated B^+ events as the signal sample [23]. The most discriminating inputs to the neural networks are $p_T(B^+)$, $d_0(B^+)$, d_0 of the kaon or pion with respect to the B^+ decay vertex, and the projected distance of the B^+ decay vertex from the primary vertex along the B^+ transverse momentum. We select approximately 51 500 B events in the $J/\psi K^+$ decay channel, 40 100 in the $\bar{D}^0\pi^+$ channel, and 11 000 in the $\bar{D}^0\pi^+\pi^+\pi^-$ channel.

To select B^{**0} mesons, three additional neural networks are trained on a combination of a simulated signal sample and real data for a background sample. The data for the background sample are taken from the entire Q range of 0 to 1000 MeV/c^2, which includes only a small contribution from the signal in the data. To avoid biasing the network training, the simulated events are generated with the same Q distribution as

the data. The B^{**0} neural networks use the same inputs as the B^+ neural networks, together with the kinematic and particle identification quantities for the pion from the B^{**0} decay. The most important discriminants are the p_T and d_0 of the pion from the B^{**0} decay vertex and the output of the B^+ neural network.

For each B^+ decay channel, we require fewer than six B^{**0} candidates in an event in order to enhance the signal-to-background ratio. The observed B^{**0} signals are consistent for all three B^+ decay channels. Therefore we combine the B^{**0} events for all decay channels and use this combined Q distribution to measure the B^{**0} properties. We count the number of Monte Carlo signal events, N_{MC}, and the number of signal and background events in the data, N_{data}, in the Q signal region of 200 to 400 MeV/c^2 for a given cut on each of the three network outputs. We then optimize the B^{**0} selection for each B^+ decay channel to maximize the combined significance, $N_{MC}/\sqrt{N_{data}}$. The resulting combined Q distribution is shown in Figure 1.

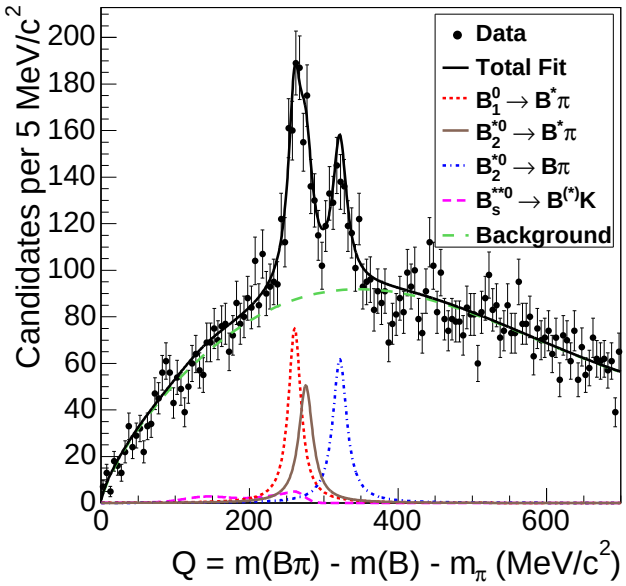

Figure 1: Distribution of the mass difference $Q = m(B^+\pi^-) - m(B^+) - m_\pi$ for exclusive B^+ decays. Curves are shown separately for the background, the $B_s^{**0} \to B^{(*)}K$ reflections, and the three B^{**0} decays.

The B^{**0} signal structure is interpreted as resulting from the three signal processes $B_1^0 \to B^{*+}\pi^-$, $B_2^{*0} \to B^+\pi^-$, and $B_2^{*0} \to B^{*+}\pi^-$, with $B^{*+} \to B^+\gamma$. The Q distribution for each signal process is modeled by a non-relativistic fixed-width Breit-Wigner function convoluted with the detector resolution model. The resolution on Q is determined from simulation and modeled as a sum of two Gaussian distributions, a dominant narrow core and a broad tail with Q-dependent standard deviations of about 2 MeV/c^2 and 4 MeV/c^2, respectively. The fraction of events in the broad tail is fixed to be 0.2.

We perform an unbinned maximum-likelihood fit to the combined Q distribution, from which we extract the Q value of the $B_2^{*0} \to B^+\pi^-$ decay, the mass difference between the B_1^0 and B_2^{*0} states, the width of the B_2^{*0}, and the number of events in each signal process. The following parameters in the fit are constrained to their values from either previous measurements or theoretical predictions: the energy of the B^{*+} decay photon, $E(\gamma) = 45.78 \pm 0.35$ MeV/c^2 [1]; the ratio of the B_1^0 and B_2^{*0} widths, $\frac{\Gamma(B_1^0)}{\Gamma(B_2^{*0})} = 0.9 \pm 0.2$ [7]; and the ratio of the B_2^{*0} branching fractions, $\frac{BR(B_2^{*0}\to B^+\pi^-)}{BR(B_2^{*0}\to B^{*+}\pi^-)} = 1.1 \pm 0.3$ [11], consistent with the value measured in Ref. [13].

The background is modeled by a sum of two components, each being the product of a power law and an exponential function. We also expect reflections from $B_s^{**0} \to B^+K^-$ decays when the kaon is mistakenly assigned the pion mass. The shape of the reflection in the Q distribution is determined in simulations of B_s^{**0} states [22] and fixed in the fit. The normalization of the B_s^{**0} is obtained by correcting the observed yield from Ref. [22] by a ratio of efficiencies to reconstruct a B_s^{**0} decay as a B^{**0} and B_s^{**0}. In the B^{**0} data sample we expect 24 ± 12 B_{s1}^0 events and 62 ± 31 B_{s2}^{*0} events. These normalizations enter the fit as Gaussian constraints.

Sources of systematic uncertainty on the mass difference and width measurements include mass scale, mass-dependent signal efficiency, fit model bias, assumptions entered as Gaussian constraints in the fit, choice of background and resolution models, and location and amount of B^{**0} broad signals. The systematic uncertainties are sum-

marized in Table 1.

To determine the mass scale uncertainty, we reconstruct $\psi(2S) \to J/\psi\pi^+\pi^-$ with $J/\psi \to \mu^+\mu^-$, which has a similar Q value as the B^{**0} decays. We compare the measured Q to the world average [1] and take the difference as the mass scale uncertainty. To evaluate the effect of signal efficiency with changing Q, we generate a large number of samples of the same size as the data, called pseudoexperiments, with the Q-dependent efficiency obtained from simulation. We then apply the default fit to the pseudoexperiments.

Tests of the fit model on pseudoexperiments show a small fit bias on the B^{**0} signal parameters, which is included as a systematic uncertainty. Signal parameters entered as Gaussian constraints in the fit contribute to the fit uncertainty. To determine their systematic contribution, we refit the data with these constrained parameters fixed. This fit returns the statistical fit uncertainties, which are subtracted in quadrature from the total fit uncertainties to obtain the systematic contribution.

To estimate the uncertainties due to the choice of background and resolution models, we generate pseudoexperiments with varied background parameterizations or worse mass resolution. The background is also well-modeled by the sum of a broad Breit-Wigner function with the product of a power law and an exponential function. From comparisons of the detector resolution in data and Monte Carlo for the $\psi(2S)$ sample, we expect the Monte Carlo to underestimate the resolution by no more than 20%. These pseudoexperiments are fit with the default fit and the generating model. The distribution of the differences between these fit results is modeled by a Gaussian, whose mean is assigned as the systematic uncertainty.

Possible effects from B_0^* and B_1' decays to our background model are studied by adding two Breit-Wigner functions of identical width varied over the range $100 - 200$ MeV/c^2. The Q values of the states are independently varied in the range 240 to 360 MeV/c^2, the region around the narrow B^{**0} peaks. We refit the data for various

Table 1: Systematic uncertainties on the B^{**0} parameter measurements. Each row corresponds to one source of systematic uncertainty. The columns show the uncertainties for each of the three B^{**0} signal parameters. Uncertainties are in units of MeV/c^2.

Source	$Q(B_2^{*0})$	$\Gamma(B_2^{*0})$	$m(B_2^{*0}) - m(B_1^0)$
Mass scale	± 0.2	–	< 0.01
Efficiency	$^{+0}_{-0.03}$	$^{+0.4}_{-0}$	$^{+0}_{-0.3}$
Fit bias	$^{+0}_{-0.1}$	$^{+0.4}_{-0}$	$^{+0}_{-0.2}$
Fit constraints	$^{+0.4}_{-0.3}$	$^{+2.1}_{-1.5}$	$^{+0.7}_{-0.9}$
Background	$^{+0.2}_{-0}$	$^{+0}_{-1.6}$	$^{+0.2}_{-0}$
Resolution	< 0.01	$^{+0}_{-0.4}$	< 0.01
Broad states	$^{+0.7}_{-0.5}$	$^{+2.3}_{-9.9}$	$^{+0.9}_{-1.0}$
Total	$^{+0.9}_{-0.7}$	$^{+3.2}_{-10.2}$	$^{+1.2}_{-1.4}$

masses and widths of the broad states, with the normalizations of the broad Breit-Wigner functions as additional free parameters in the fit model. We then take the largest variation in the narrow B^{**0} parameters from any configuration of broad states as the systematic uncertainty due to the B^{**0} broad states.

The result of the likelihood fit to the data is shown in Figure 1, and we measure the following:

$$m(B_2^{*0}) - m(B^+) - m_\pi = 321.5^{+1.7}_{-1.8}(\text{stat.})^{+0.9}_{-0.7}(\text{syst.})\ \text{MeV}/c^2;$$

$$m(B_2^{*0}) - m(B_1^0) = 14.9^{+2.2}_{-2.5}(\text{stat.})^{+1.2}_{-1.4}(\text{syst.})\ \text{MeV}/c^2; \text{ and}$$

$$\Gamma(B_2^{*0}) = 22.7^{+3.8}_{-3.2}(\text{stat.})^{+3.2}_{-10.2}(\text{syst.})\ \text{MeV}/c^2.$$

The signal is consistent with theoretical predictions [5, 6], and Gaussian-constrained parameters remain close to their input values, the largest departure being 0.4 standard deviations. The event numbers are $N(B_1^0) = 503^{+75}_{-68}$, $N(B_2^{*0} \to B^+\pi^-) = 385^{+48}_{-45}$, and $N(B_2^{*0} \to B^{*+}\pi^-) = 351^{+48}_{-45}$, where uncertainties are statistical only. Using the mass of the B^+ [1] and the correlations between the fit parameters, the masses

of the B_1^0 and B_2^{*0} are $m(B_2^{*0}) = 5740.2^{+1.7}_{-1.8}(\text{stat.})^{+0.9}_{-0.8}(\text{syst.})$ MeV/c^2 and $m(B_1^0) = 5725.3^{+1.6}_{-2.2}(\text{stat.})^{+1.4}_{-1.5}(\text{syst.})$ MeV/c^2. With the current statistics the data are also consistent with containing only the B_1^0 and $B_2^{*0} \to B^+\pi^-$ peaks.

In summary, using the three fully reconstructed decays $B^+ \to J/\psi K^+$, $B^+ \to \bar{D}^0\pi^+$, and $B^+ \to \bar{D}^0\pi^+\pi^+\pi^-$, we observe two narrow B^{**0} states in the decays $B_1^0 \to B^{*+}\pi^-$ and $B_2^{*0} \to B^{(*)+}\pi^-$. This is the most precise measurement of the narrow B^{**0} masses to date. We have also measured the B_2^{*0} width for the first time. There is some discrepancy between these measurements and those reported by the D0 collaboration [13], the largest being close to a 3 σ difference in the mass splitting of the two B^{**0} states.

We thank the Fermilab staff and the technical staffs of the participating institutions for their vital contributions. This work was supported by the U.S. Department of Energy and National Science Foundation; the Italian Istituto Nazionale di Fisica Nucleare; the Ministry of Education, Culture, Sports, Science and Technology of Japan; the Natural Sciences and Engineering Research Council of Canada; the National Science Council of the Republic of China; the Swiss National Science Foundation; the A.P. Sloan Foundation; the Bundesministerium für Bildung und Forschung, Germany; the Korean Science and Engineering Foundation and the Korean Research Foundation; the Science and Technology Facilities Council and the Royal Society, UK; the Institut National de Physique Nucleaire et Physique des Particules/CNRS; the Russian Foundation for Basic Research; the Ministerio de Ciencia e Innovación, Spain; the Slovak R&D Agency; and the Academy of Finland.

References

[1] C. Amsler *et al.* (Particle Data Group), Phys. Lett. B **667**, 1 (2008).

[2] N. Isgur and M. B. Wise, Phys. Lett. B **232**, 113 (1989); *ibid.* B **237**, 527 (1990).

[3] E. J. Eichten, C. T. Hill, and C. Quigg, Phys. Rev. Lett. **71**, 4116 (1993); E. J. Eichten, C. T. Hill, and C. Quigg, FERMILAB-CONF-94/118-T (1994).

[4] N. Isgur, Phys. Rev. D **57**, 4041 (1998).

[5] D. Ebert, V. O. Galkin, and R. N. Faustov, Phys. Rev. D **57**, 5663 (1998) [*Erratum-ibid.* D **59**, 019902 (1999)].

[6] T. Matsuki, T. Morii, and K. Sudoh, Prog. Theor. Phys. **117**, 1077 (2007).

[7] A. F. Falk and T. Mehen, Phys. Rev. D **53**, 231 (1996).

[8] A. H. Orsland and H. Hogaasen, Eur. Phys. J. C **9**, 503 (1999).

[9] T. Mehen, private communication.

[10] R. Akers *et al.* (OPAL Collaboration), Z. Phys. C **66**, 19 (1995); P. Abreu *et al.* (DELPHI Collaboration), Phys. Lett. B **345**, 598 (1995); D. Buskulic *et al.* (ALEPH Collaboration), Z. Phys. C **69**, 393 (1996); M. Acciarri *et al.* (L3 Collaboration), Phys. Lett. B **465**, 323 (1999); A. Affolder *et al.* (CDF Collaboration), Phys. Rev. D **64**, 072002 (2001).

[11] A. Oyanguren (DELPHI Collaboration), *Proceedings of 32nd International Conference on High-Energy Physics (ICHEP 04), Beijing, China, 16-22 Aug 2004*. Hackensack, World Scientific (2005), 2 vols.

[12] R. Barate *et al.* (ALEPH Collaboration), Phys. Lett. B **425**, 215 (1998).

[13] V. M. Abazov *et al.* (D0 Collaboration), Phys. Rev. Lett. **99**, 172001 (2007).

[14] D. Acosta *et al.* (CDF Collaboration), Phys. Rev. D **71**, 032001 (2005).

[15] C. S. Hill, Nucl. Instrum. Methods A **530**, 1 (2004); A. Affolder *et al.*, *ibid.* A **453**, 84 (2000); A. Sill, *ibid.* A **447**, 1 (2000).

[16] T. Affolder *et al.*, Nucl. Instrum. Methods A **526**, 249 (2004).

[17] G. Ascoli *et al.*, Nucl. Instrum. Methods A **268**, 33 (1988).

[18] E. J. Thomson *et al.*, IEEE Trans. Nucl. Sci. **49**, 1063 (2002).

[19] W. Ashmanskas *et al.*, Nucl. Instrum. Methods A **518**, 532 (2004).

[20] A. Abulencia *et al.* (CDF Collaboration), Phys. Rev. Lett. **96**, 191801 (2006).

[21] M. Feindt, arXiv:physics/0402093 (2004); M. Feindt and U. Kerzel, Nucl. Instrum. Methods A **559**, 190 (2006).

[22] T. Aaltonen *et al.* (CDF Collaboration), Phys. Rev. Lett. **100**, 082001 (2008).

[23] We use several single b hadron simulations, all using the B-hadron $p_{\rm T}$ and y distributions obtained from B decays in CDF Run II data. The b hadron decays are generated with the EvtGen package, D. J. Lange, Nucl. Instrum. Methods A **462**, 152 (2001). Monte Carlo samples that also contain the hadronization backgrounds were generated by the pythia program, T. Sjöstrand *et al.*, Comput. Phys. Commun. **135**, 238 (2001).